Published in final edited form as:

J Biomed Nanotechnol. 2016 April ; 12(4): 753–761.

Bio-Templated Growth of Bone Minerals from Modified Simulated Body Fluid on Nanofibrous Decellularized Natural Tissues

Mingying Yang[1,*,†], **Jie Wang**[1,†], **Ye Zhu**[2], and **Chuanbin Mao**[2,3,*]

[1]Institute of Applied Bioresource Research, College of Animal Science, Zhejiang University, Hangzhou, Zhejiang 310058, China

[2]Department of Chemistry and Biochemistry, Stephenson Life Sciences Research Center, University of Oklahoma, Norman, OK 73019, USA

[3]School of Materials Science and Engineering, Zhejiang University, Hangzhou, Zhejiang 310027, China

Abstract

Small intestine submucosal (SIS) membrane used in this study is a decellularized, naturally occurring nanofibrous scaffold derived from a submucosal layer of porcine small intestine. It is predominantly composed of type I collagen fibers. Here we studied the bio-templated growth of hydroxylapatite (HAP) bone minerals on the SIS membrane from a modified simulated body fluid (1.5 SBF) at the body temperature, namely, under a near-physiological condition, in order to evaluate its bone bioactivity, the capability of the membrane in bonding with bone tissue once implanted *in vivo*. Minute HAP crystals were successfully nucleated on the SIS membranes from 1.5 SBF at the body temperature. The crystals were preferentially nucleated along the collagen fibers constituting the SIS membranes. HAP was the major crystalline mineral phase formed during the whole period of time and a minor crystalline phase of tricalcium phosphate (TCP) appeared after the membranes were incubated for 96 h. We also found that the mineralization for 8 h most significantly promoted the osteogenic differentiation of rat mesenchymal stem cells (MSCs) by evaluating the formation of osteogenic markers in MSCs including alkaline phosphatase (early stage marker) as well as osteocalcin and osteopontin (late stage markers). Hence, SIS membranes show excellent bone bioactivity and once mineralized, can significantly promote the osteogenic differentiation of MSCs.

Keywords

Nanofibers; Biomineralization; Tissues; Hydroxyapatite; Mesenchymal Stem Cells

[*]Authors to whom correspondence should be addressed. yangm@zju.edu.cn, cbmao@ou.edu.
[†]These two authors contributed equally to this work.

INTRODUCTION

Hydroxyapatite [HAP, $Ca_{10}(PO_4)_6(OH)_2$] is one of the most important calcium orthophosphates in natural environment. It represents the main mineral component in bone tissue and exists in the form of minute crystals in bone. Thus HAP has received great attention in hard tissue regeneration and has been used worldwide as a bone substitute.[1] Bone biomineralization involves the deposition of HAP crystals along the nanoscale type I collagen fibers that self-assemble into and constitute an extracellular matrix (ECM). We, along with others, have used different nanoscale bio-templates to induce biomimetic nucleation and growth of HAP crystals, including chemically modified 2D surfaces such as self-assembled monolayers and fiber-like macromolecules such as filamentous phage and silk.[2–5] Type I collagen is an attractive molecule for manufacturing bone biomaterials because it forms the major organic component in bone ECM. Composites made of HAP crystals and type I collagen fibers show great promise as biomaterials for bone tissue engineering since bone is a natural composite primarily composed of cells and ECM made of these two components. Ideally, a scaffold for bone tissue engineering should resemble ECM in bone. One approach to this goal is the deposition of HAP crystals on the collagen fibers that are already preassembled into a matrix.

Porcine small intestine submucosal (SIS) membrane used in this work is a decellularized, naturally occurring tissue matrix composed of collagen fibers and various growth factors. It is derived from the porcine jejunum, contains a 3-dimensional (3D) nanofibrous structure, and has a complex composition predominantly composed of type I collagen fibers. In SIS membranes, collagen fibers are almost parallel to each other (Figs. 1(a)–(b)). *In vivo* studies indicated that SIS membranes could be rapidly absorbed and support early and abundant new vessel growth, and thus could be a useful biomaterial for the repair of several tissues including large vascular grafts, venous valves and leaflets, ligaments, tendons, abdominal wall, skin, urinary bladder and biliary tract.[6–8] However, to the best of our knowledge, the use of SIS membranes in *in vivo* bone regeneration has not been demonstrated.

Recently, we found that SIS membranes could induce the HAP mineralization from a calcium phosphate solution supersaturated with respect to HAP, which was made by dissolving HAP under an acidic condition, at the room temperature. However, the biomineralization under such a non-physiological condition resulted in the formation of HAP on the SIS membranes partially due to the super-saturation of HAP in the solution. Since the previous results of mineralization on the SIS membranes were obtained from the non-physiological condition, they do not necessarily indicate that the SIS membranes are capable of inducing biomineralization under a physiological condition to promote their bonding with bone tissue when implanted *in vivo*. It is well-known that mineralization from a simulated body fluid (SBF) or its modified version at the body temperature is a powerful approach for evaluating the bone bioactivity of a biomaterial *in vitro* (i.e., its ability to bond with bone tissue) without animal experiments since SBF or modified SBF at the body temperature mimics the physiological condition. Therefore, to evaluate whether SIS membranes have excellent bone bioactivity, herein, we studied the biomineralization of HAP on the SIS membranes in a modified SBF (1.5 SBF, Table I) at the body temperature, which represents a near-physiological condition. Scheme 1 illustrates the nanofibrous collagenous

structure of the SIS membranes and the principle of the biomimetic mineralization on the membranes. On the other hand, this study also generated biomineralized SIS membranes while evaluating the bone bonding capability of the SIS membranes. We expect that the biomineralized SIS membranes are better scaffolds than non-mineralized ones for bone tissue engineering because they mimic both chemical composition and fibrous architecture of the ECM of bone tissue and have the potential to behave as natural bone ECM in bone regeneration. In addition, we recently found that HAP mineralization promoted the osteogenic differentiation of MSCs.[9] Therefore, we further evaluated whether the biomineralized SIS membranes formed under the near-physiological condition could promote osteogenic differentiation of MSCs.

MATERIALS AND METHODS

Mineralization of SIS Membranes in 1.5 SBF

The modified SBF, 1.5 SBF, was prepared following a reported protocol. Briefly, 700 ml of ion-exchanged and distilled water was first added into a 1,000 ml plastic beaker. The beaker was then placed in a water bath and heated to 36.5 ± 1.5 °C under magnetic stirring. Then the reagents listed in Table I were dissolved into the solution one by one in the order given. The pH value of the 1.5 SBF was buffered at 7.4 with 1 M of HCl and tris-(hydroxymethyl)-aminomethane [$(CH_2OH)_3CNH_2$] at 36.5 ± 1.5 °C.

Decellularized nanofibrous SIS membranes purchased from Cook Biotech were dehydrated in air and cut into small square pieces (1 cm × 1 cm). To initiate biomimetic nucleation and growth of HAP crystals, the nanofibrous SIS membranes were placed into the 1.5 SBF and incubated for up to 96 h. During the incubation, minerals were formed on the membranes due to the preferential nucleation of the minerals on the membranes (Scheme 1). The mineralized membranes were taken out of the solution after being incubated for a certain period of time, rinsed in the deionized water and then stored in a desiccator before materials characterization.

Materials Characterization

In order to study the morphologies of the crystals that were nucleated and grown on the SIS membranes by scanning electron microscopy (SEM), the samples were coated with AuPd alloy to increase surface conductivity using a Hummer VI triode sputter coater. SEM images were observed with ZEISS DSM-960A scanning electron microscope and taken using IXRF software. The phase composition of the crystals grown on the SIS membranes was determined by X-ray diffraction (XRD) on a Scintag X2 diffractometer. The pH value of the mineralization solution where the SIS membranes were incubated was monitored *in situ* with UltraBASIC UB-10 pH/mV numeric acidity meter.

Culture of Rat MSCs on Mineralized SIS Membranes

We cultured mesenchymal stem cells (MSCs) isolated from rats in the osteogenic differentiation media on the SIS membranes with different mineralization times following our published protocols.[9] Briefly, the MSCs were expanded in the primary media, which contained Dulbecco's Modified Eagle Media (DMEM, Gibco), 15% fetal bovine serum

(FBS, Gibco) and 1% antibiotics (penicillin 100 U/ml, streptomycin 100 U/ml). When the cells reached the passage, they were seeded onto the SIS membranes and then cultured in the osteogenic differentiation media (Thermo scientific). The cell culture media was replaced twice a week.

Proliferation of MSCs on Mineralized SIS Membranes

We employed 3-(4,5-dimethylthiazol-2-yl)-2,5-diphenyl tetrazolium bromide (MTT) assay to evaluate the proliferation on the SIS membranes at the different time points.[,] Briefly, the cell-SIS complex was incubated in the MTT solution (20 μl, 5 mg/ml) at 37 °C in a 5% CO_2 incubator for 4 h. The cell metabolism would produce intense purple formazan derivative, which was first eluted and then dissolved in 150 μl of dimethylsulfoxide (DMSO) per well of a plate. Finally, the absorbance at 490 nm was measured using a microplate reader.

Osteogenic Differentiation of MSCs on Mineralized SIS Membranes

Alkaline phosphatase (ALP) as well as osteocalcin (OCN) and osteopontin (OPN) are marker proteins specific for the early and late stage of osteogenic differentiation of MSCs, respectively.[,] ALP is an enzyme and thus the formation of this marker has been commonly evaluated by detecting its activity. Specifically, because ALP could modify a substrate (called *p*-nitrophenol phosphate) to produce a yellow product (called *p*-nitrophenol), the amount of the produced yellow product would indicate the amount of ALP formed due to the osteogenic differentiation of MSCs. The ALP assay was carried out following a protocol reported by us previously. Moreover, in order to verify the osteogenic differentiation of MSCs at late stage, real-time polymerase chain reaction (PCR) analysis was used to characterize the gene expression of OCN and OPN by following our published protocol.[,] The sequences of the primers designed for PCR could be found in our pervious publications as well.[,]

Statistical Analysis

The data of cell proliferation and differentiation were presented as mean values ± standard deviation. SPSS Statistics software was employed to conduct statistical analysis. Differences between two groups were considered significant at $p < 0.05$.

RESULTS

Morphologies of Mineral Crystals Grown on Nanofibrous SIS Scaffolds

After mineralization of the SIS membranes, SEM images (Fig. 1) indicate that the crystals were nucleated on the membranes. The crystals were packed densely on the SIS membranes mineralized in 1.5 SBF. The nucleation and growth of HAP crystals on the SIS membranes were very rapid and most of the crystals were grown in the first half an hour (Figs. 1(c)–(d)). The crystals were polygonal with sizes ranging from 1 to 2.5 μm and loosely packed on the surface of SIS membranes during the first half hour. The polygonal crystals were packed more densely and fused into irregular larger crystals after 8 h (Figs. 1(e)–(f)). After incubation for 24 h, the morphologies of the grown crystals changed from more well-defined (polygonal) to less defined (Figs. 1(g)–(h)); the sharp corners of the polygons became more round, indicating the partial dissolution of the crystals at the corners, which might arise from

the higher surface energy state of the corners than other surface areas of the crystals. This resulted in the fusion of crystals into a larger aggregate. After mineralization for 96 h, some of the crystals were dissolved and the number of crystals was reduced (Figs. 1(i)–(j)).

Phase Composition of Crystals Grown on SIS Biotemplates

Figure 2 depicts the XRD patterns of the SIS membranes after mineralization. The SIS membrane before mineralization did not show any crystalline diffraction peaks (data not shown). On the mineralized SIS membranes, HAP was the major crystalline phase present during the whole period of mineralization. Typical peaks at 28.6°, 31.7°, and 45.5° were observed from all patterns and are corresponding to the crystal planes (210), (211), and (203) of HAP, respectively. A comparison of the XRD patterns between different mineralization times showed that the SIS membranes mineralized for 8 h presented the highest HAP diffraction signals (Fig. 2(B)), indicating that mineralization for 8 h led to the highest content of HAP on the SIS membranes. However, under the non-physiological condition (in HAP-supersaturated solutions and at room temperature), the HAP formation reached the highest content at 24 h, suggesting that the mineralization from 1.5 SBF, namely, under the near-physiological condition, is faster. After the SIS membranes were incubated in 1.5 SBF for 96 h, there appeared an obvious small peak at 27.4° that could be attributed to tricalcium phosphate (TCP) crystal structure (Fig. 2(D)), indicating that TCP was a minor crystalline phase co-existing with the major phase HAP. This phase was not found in the biomineralization under the non-physiological condition. In fact, TCP is a desired mineral phase in bone biomaterials and often is used as a component to form a composite with HAP as a bone implant because it promotes the bone resorption *in vivo* and is known as a "bone-rebuilding material." In this sense, the mineral structure formed under the physiological condition, as reported in this work, is more suitable than that formed under the non-physiological condition.

pH Changes of the Mineralization Solutions

By monitoring the pH values of the mineralization solutions as a function of mineralization time, we found that the pH value of the 1.5 SBF solution remains nearly unchanged, which is due to the buffering capability of 1.5 SBF. However, our earlier studies showed that biomineralization from HAP-supersaturated solutions would reduce the pH values over the process of HAP formation because HAP formation consumed OH^- ions. Even though HAP formation will consume OH^- ions as well (Scheme 1), the buffering capability of the 1.5 SBF ensures that the pH value of the mineralization solution will not change significantly. This result shows that 1.5 SBF is indeed a good mineralization solution for evaluating the biomineralization on the SIS membranes.

Proliferation of MSCs on the Mineralized Nanofibrous SIS Membranes

We used MTT assay to evaluate the proliferation of MSCs cultured on the SIS membranes mineralized for different times (0, 0.5, 8, 24, and 96 h). We found that for each substrate, the cell number, reflected by the optical density (OD) at 490 nm, was increased over the time (Fig. 3). More importantly, SIS membranes mineralized for 8 h, which presented the highest mineral content among all mineralized substrates (Fig. 2), showed the lowest proliferation rate (Fig. 3). The difference in the proliferation rate may imply the difference in osteogenic

differentiation rate because there seems to be an inverse relationship between the rate of proliferation and osteogenic differentiation of MSCs.[–] This implication was actually confirmed by the osteogenic differentiation results described below.

Osteogenic Differentiation of MSCs on Mineralized Nanofibrous SIS Membranes

The ALP activity, normalized to the cell number of the respective sample, showed that biomineralization of SIS membranes in 1.5 SBF elevated the ALP activity and thus promoted the osteogenic differentiation of MSCs in comparison to the non-mineralized SIS membranes ($p < 0.05$, Fig. 4(a)). Moreover, as expected from the aforementioned proliferation study, ALP activity showed that the SIS membranes mineralized in 1.5 SBF for 8 h was the best in promoting the osteogenic differentiation (Fig. 4(a)). Our XRD patterns showed that mineralization in 1.5 SBF for 8 h resulted in the highest content of HAP (Fig. 2(B)). Therefore, it is likely that it is the highest content of HAP in the SIS membranes that allowed the SIS membranes mineralized for 8 h to achieve the best capability in promoting the osteogenic differentiation of MSCs. By considering the slowest proliferation rate for the SIS membranes mineralized for 8 h (Fig. 3), our study verified the inverse relationship between proliferation and osteogenic differentiation of MSCs, which was in agreement with the reported studies.[–] Real-time PCR analysis also showed that the biomineralization of SIS membranes up-regulated the gene expression level of OCN (Fig. 4(b)) and OPN (Fig. 4(c)), and thus promoted the osteogenic differentiation of MSCs. It also showed that the SIS membranes mineralized for 8 h had the highest level of OCN and OPN expression, suggesting that they were most capable of promoting the osteogenic differentiation of MSCs among all mineralized substrates (Fig. 4). Therefore, both ALP activity assay and real-time PCR analysis consistently verified that the biomineralization of SIS membranes promoted the osteogenic differentiation of MSCs when cultured on the SIS membranes. These results are in agreement with earlier findings that the addition of bone mineral (HAP) to the scaffolds, arising from the biomineralization, could promote the osteogenic differentiation of MSCs and bone formation.[, –]

DISCUSSION

Our previous work showed that the SIS membranes could induce the formation of HAP under a non-physiological condition. This study made a further step to explore the possibility of HAP mineralization on the SIS membranes under a physiological condition in order to predict whether the implantation of the SIS membranes *in vivo* could induce HAP formation on the SIS membranes to achieve the optimal bonding between the membranes and the surrounding bone tissues. Namely, the major goal is to test whether the SIS membranes can induce biomineralization in body fluid under physiological conditions. By using the 1.5 SBF as a mineralization solution mimicking body fluid, instead of the non-physiological HAP-supersaturated solution, we successfully showed that the SIS membranes alone could induce the formation of HAP from a near-physiological media at the body temperature, suggesting the excellent bone bioactivity of the SIS membranes. It is well-accepted that evaluating whether a biomaterial can promote the formation of HAP in SBF or modified SBF at the body temperature is a common *in vitro* approach to predicating the *in*

vivo bone bioactivity of this biomaterial, namely, the ability of the biomaterial to bond with bone.

Moreover, this study demonstrated that biomineralization under near-physiological conditions on the SIS membranes led to the formation of biomineralized scaffolds. Namely, the SIS membranes could serve as a template for the biomimetic nucleation and growth of HAP crystals, generating a scaffold for bone tissue engineering with composition and structure closely resembling those of natural bone. Our SEM images showed that the microstructure of the SIS membranes used in our experiment was composed of collagen fibers that were almost parallel to each other (Fig. 1(a)), which is consistent with the reported structure.[,] In the present study, because collagen fibers were densely packed into SIS membranes, it was difficult to resolve all of individual fibers on the surface. However, in some surface area, individual fibers could be resolved, allowing us to use SEM images to show that the grown crystals were preferentially distributed along those fibers (Fig. 1). These results are in agreement with the fact that HAP crystals are nucleated and organized along the collagen fibers in natural bone, indicating biomimetic nucleation and growth on the constituent collagen fibers in our SIS membranes. SEM results obtained from the present study demonstrated that the collagen fibers in the SIS membranes could mimic those in bone to nucleate HAP crystals in 1.5 SBF. Our results have proved that the nucleation and growth of HAP crystals on the SIS membranes under the near-physiological condition can effectively mimic the biological mineralization processes due to the templating effect of the collagen fibers in the SIS membranes.

Apatite formation is a complex process and nucleation and growth of HAP crystals can be affected by several factors such as the concentration of the precursors and the type of templates.[–] It is reported that amorphous calcium phosphate (ACP) will be formed first at a highly supersaturated calcium phosphate solution, followed by the conversion of ACP into HAP.[,] Since non-mineralized SIS membranes are amorphous, it is difficult to judge the formation of ACP at the very beginning of the mineralization by using XRD. However, according to the reported theory,[,] it is likely that the HAP crystals formed on the SIS membranes were rapidly converted from ACP formed at the very beginning of the biomimetic mineralization. Previous studies[,] have also demonstrated that both HAP-supersaturated solution and 1.5 SBF can induce heterogeneous nucleation when the solution is in direct contact with a foreign substrate. Once the apatite nuclei are formed, they grow by uptake of calcium and phosphate ions from the solution.[,]

After a period of mineralization for 24 h, the sharp corners of the polygonal crystals became round (Fig. 1), indicating the partial dissolution of crystals at the corners and resulting in the fusion of crystals into a larger aggregate. The partial dissolution of the HAP crystals led to not only the morphological changes (Figs. 1(g)–(j)) but also the decrease in the intensity of diffraction peaks in the XRD patterns (Figs. 2(C)–(D)). It has been demonstrated that HAP can be converted to TCP.[–] The appearance of TCP on the SIS membranes after 96 h in 1.5 SBF may be due to the conversion of dissolved HAP into TCP.

A variety of biomimetic materials have been shown to promote osteogenic differentiation of stem cells.[–] For example, Leong et al. demonstrated that scaffolds made from materials that

were of a close stiffness to bone could favor the osteogenic differentiation of stem cells.[–] Although the mineralized SIS membranes are composed of two components (SIS and HAP) with proved biocompatibility, whether the composites of SIS membranes and HAP formed due to the biomineralization of the SIS membranes in 1.5 SBF could promote the osteogenic differentiation of MSCs has never been reported previously. In this work, we statistically compared the difference in the osteogenic differentiation of MSCs on five groups, namely, the SIS membranes mineralized for 0, 0.5, 8, 24, and 96 h (Fig. 4). Such comparison showed that the SIS membranes mineralized in 1.5 SBF showed better capability in promoting the osteogenic differentiation of MSCs needed for bone formation than the non-mineralized SIS membranes (Fig. 4). In particular, it further proved that among the biomineralized SIS membranes, those derived from the biomineralization for 8 h achieved the best capability in promoting the osteogenic differentiation of MSCs. Our findings are consistent with our recently discovery that the HAP mineralization on natural protein scaffolds can promote the osteogenic differentiation of MSCs.[,] Therefore, our work implies that the SIS membranes can be mineralized in body fluids under the physiological condition, and once mineralized, will further promote *in vivo* bone formation. Evaluating the use of SIS membranes in *in vivo* bone regeneration is now underway in our group.

CONCLUSIONS

We have successfully demonstrated that the SIS membranes can induce biomineralization from 1.5 SBF at body temperature, namely, under a near-physiological condition. The process of biomimetic mineralization from 1.5 SBF is found to be similar to the biological mineralization of bone in that HAP tends to be nucleated and grown on the collagen fibers. The successful biomineralization under the near-physiological condition further shows that the SIS membranes have excellent bone bioactivity and indicate that they will be able to bond with bone tissues once implanted *in vivo*. Our work has also proved that the biomineralization under the near-physiological condition can further promote the osteogenic differentiation of stem cells, which will promote bone regeneration *in vivo*. In addition, we found that the biomineralization for 8 h is the best for achieving the most efficient osteogenic differentiation of the stem cells.

Acknowledgments

We would like to thank the financial support from National Institutes of Health (EB015190), National Science Foundation (CBET-0854465, CMMI-1234957, CBET-0854414, and DMR-0847758), Department of Defense Peer Reviewed Medical Research Program (W81XWH-12-1-0384), Oklahoma Center for Adult Stem Cell Research (434003) and Oklahoma Center for the Advancement of Science and Technology (HR14-160). Mingying Yang also thanks the generous support from National Natural Science Foundation of China (21172194), Projects of Zhejiang Provincial Science and Technology Plans (2012C12910), Silkworm Industry Science and Technology Innovation Team (2011R50028), China Agriculture Research System (CARS-22-ZJ0402), and National High Technology Research and Development Program 863 (2013AA102507).

REFERENCES

1. Weiner S, Wagner HD. The material bone: Structure-mechanical function relations. Annu. Rev. Mater. Sci. 1998; 28:271.
2. Tan KK, Tan GH, Shamsul BS, Chua KH, Ng MHA, Ruszymah BHI, Aminuddin BS, Loqman MY. Bone graft substitute using hydroxyapatite scaffold seeded with tissue engineered autologous osteoprogenitor cells in spinal fusion: Early result in a sheep model. Med. J. Malay. 2005; 60:53.

3. White SW, Hulmes DJS, Miller A, Timmins PA. Collagen mineral axial relationship in calcified turkey leg tendon by X-ray and neutron diffraction. Nature. 1977; 266:421. [PubMed: 859610]
4. Wang X, Grogan SP, Rieser F, Winkelmann V, Maquet V, Berge ML, Mainil-Varlet P. Tissue engineering of biphasic cartilage constructs using various biodegradable scaffolds: An *in vitro* study. Biomaterials. 2004; 25:3681. [PubMed: 15020143]
5. Bigi A, Boanini E, Panzavolta S, Roveri N. Biomimetic growth of hydroxyapatite on gelatin films doped with sodium polyacrylate. Biomacromolecules. 2000; 1:752. [PubMed: 11710207]
6. Boskey AL. Hydroxyapatite formation in a dynamic collagen gel system: Effects of type I collagen, lipids, and proteoglycans. J Phys. Chem. 1989; 93:1628.
7. Kim H-L, Song T-W. Formation of solution-derived hydroxyapatite layer on the surface of a shell. J Korean Ceram. Soc. 2002; 39:1177.
8. Xu H, Cao BR, George A, Mao CB. Self-assembly and mineralization of genetically modifiable biological nanofibers driven by beta-structure formation. Biomacromolecules. 2011; 12:2193. [PubMed: 21520924]
9. Wang FK, Cao BR, Mao CB. Bacteriophage bundles with prealigned Ca^{2+} initiate the oriented nucleation and growth of hydroxylapatite. Chem. Mater. 2010; 22:3630. [PubMed: 20802794]
10. He T, Abbineni G, Cao BR, Mao CB. Nanofibrous bioinorganic hybrid structures formed through self-assembly and oriented mineralization of genetically engineered phage nanofibers. Small. 2010; 6:2230. [PubMed: 20830718]
11. Mao CB, Li H, Cui F, Feng Q, Ma C. Oriented growth of phosphates on polycrystalline titanium in a process mimicking biomineralization. J Crystal Growth. 1999; 206:308.
12. Mao CB, Li H, Cui F, Feng Q, Ma C. The functionalization of titanium with edta to induce biomimetic mineralization of hydroxyapatite. J Mater. Chem. 1999; 9:2573.
13. Mao CB, Li H, Cui F, Feng Q, Wang H, Ma C. Oriented growth of hydroxyapatite on (0001) textured titanium with functionalized self-assembled silane monolayer as template. J Mater. Chem. 1998; 8:2795.
14. Yang M, Shuai Y, Zhang C, Chen Y, Zhu L, Mao CB, OuYang H. Biomimetic nucleation of hydroxyapatite crystals mediated by *antheraea pernyi* silk sericin promotes osteogenic differentiation of human bone marrow derived mesenchymal stem cells. Biomacromolecules. 2014; 15:1185. [PubMed: 24666022]
15. Cao B, Mao CB. Oriented nucleation of hydroxylapatite crystals on spider dragline silks. Langmuir. 2007; 23:10701. [PubMed: 17850102]
16. Brown-Etris RM, Cutshall WD, Hiles MC. A new biomaterial derived from small intestine submucosa and developed into a wound matrix device. Wounds. 2002; 14:150.
17. Ambro BT, Zimmerman J, Rosenthal M, Pribitkin EA. Nasal septal perforation repair with porcine small intestinal submucosa. Arch. Facial Plast. Surg. 2003; 5:528. [PubMed: 14623693]
18. Badylak S, Kokini K, Tullius B, Simmons-Byrd A, Morff R. Morphologic study of small intestinal submucosa as a body wall repair device. J Surg. Res. 2002; 103:190. [PubMed: 11922734]
19. Badylak SF, Lantz GC, Coffey A, Geddes LA. Small intestinal submucosa as a large diameter vascular graft in the dog. J Surg. Res. 1989; 47:74. [PubMed: 2739401]
20. Badylak SF, Tullius R, Kokini K, Shelbourne KD, Klootwyk T, Voytik SL, Kraine MR, Simmons C. The use of xenogeneic small intestinal submucosa as a biomaterial for achilles tendon repair in a dog model. J Biomed. Mater. Res. 1995; 29:977. [PubMed: 7593041]
21. Brountzos E, Pavcnik D, Timmermans HA, Corless C, Uchida BT, Nihsen ES, Nakata M, Schoder M, Kaufman JA, Keller FS, Rosch J. Remodeling of suspended small intestinal submucosa venous valve: An experimental study in sheep to assess the host cells' origin. J Vasc. Interv. Radiol. 2003; 14:349. [PubMed: 12631640]
22. Bussieres M, Krohne SG, Stiles J, Townsend WM. The use of porcine small intestinal submucosa for the repair of full-thickness corneal defects in dogs, cats and horses. Vet. Ophthalmol. 2004; 7:352. [PubMed: 15310296]
23. Caione P, Capozza N, Zavaglia D, Palombaro G, Boldrini R. *In vivo* bladder regeneration using small intestinal submucosa: Experimental study. Pediatr. Surg. Int. 2006; 22:593. [PubMed: 16773371]

24. Cheng EY, Kropp BP. Urologic tissue engineering with small intestinal submucosa: Potential clinical applications. World J. Urol. 2000; 18:26. [PubMed: 10766040]
25. Colvert JR 3rd, Kropp BP, Cheng EY, Pope JCT, Brock JW 3rd, Adams MC, Austin P, Furness PD 3rd, Koyle MA. The use of small intestinal submucosa as an off-the-shelf urethral sling material for pediatric urinary incontinence. J Urol. 2002; 168:1872. [PubMed: 12352379]
26. Duchene DA, Jacomides L, Ogan K, Lindberg G, Johnson BD, Pearle MS, Cadeddu JA. Ureteral replacement using small-intestinal submucosa and a collagen inhibitor in a porcine model. J Endourol. 2004; 18:507. [PubMed: 15253833]
27. Fox DB, Cook JL, Arnoczky SP, Tomlinson JL, Kuroki K, Kreeger JM, Malaviya P. Fibrochondrogenesis of free intraarticular small intestinal submucosa scaffolds. Tissue Eng. 2004; 10:129. [PubMed: 15009938]
28. Gabouev AI, Schultheiss D, Mertsching H, Koppe M, Schlote N, Wefer J, Jonas U, Stief CG. *In vitro* construction of urinary bladder wall using porcine primary cells reseeded on acellularized bladder matrix and small intestinal submucosa. Int. J. Artif. Organs. 2003; 26:935. [PubMed: 14636011]
29. Kropp BP, Ludlow JK, Spicer D, Rippy MK, Badylak SF, Adams MC, Keating MA, Rink RC, Birhle R, Thor KB. Rabbit urethral regeneration using small intestinal submucosa onlay grafts. Urology. 1998; 52:138. [PubMed: 9671888]
30. Lai JY, Chang PY, Lin JN. Body wall repair using small intestinal submucosa seeded with cells. J Pediatr. Surg. 2003; 38:1752. [PubMed: 14666459]
31. Badylak SF, Record R, Lindberg K, Hodde J, Park K. Small intestinal submucosa: A substrate for *in vitro* cell growth. J Biomater. Sci. Polym. Ed. 1998; 9:863. [PubMed: 9724899]
32. Campodonico F, Benelli R, Michelazzi A, Ognio E, Toncini C, Maffezzini M. Bladder cell culture on small intestinal submucosa as bioscaffold: Experimental study on engineered urothelial grafts. Eur. Urol. 2004; 46:531. [PubMed: 15363573]
33. Cimini M, Boughner DR, Ronald JA, Johnston DE, Rogers KA. Dermal fibroblasts cultured on small intestinal submucosa: Conditions for the formation of a neotissue. J Biomed. Mater. Res. A. 2005; 75:895. [PubMed: 16118790]
34. Zhang Y, Kropp BP, Moore P, Cowan R, Furness PD 3rd, Kolligian ME, Frey P, Cheng EY. Coculture of bladder urothelial and smooth muscle cells on small intestinal submucosa: Potential applications for tissue engineering technology. J Urol. 2000; 164:928. [PubMed: 10958711]
35. Zhang Y, Lin HK, Frimberger D, Epstein RB, Kropp BP. Growth of bone marrow stromal cells on small intestinal submucosa: An alternative cell source for tissue engineered bladder. BJU. Int. 2005; 96:1120. [PubMed: 16225540]
36. Yang M, Zhou G, Castano H, Zhu Y, Mao CB. Biomineralization of natural collagenous nanofibrous membranes and their potential use in bone tissue engineering. J Biomed. Nanotech. 2015; 11:447.
37. Kokubo T, Takadama H. How useful is sbf in predicting *in vivo* bone bioactivity? Biomaterials. 2006; 27:2907. [PubMed: 16448693]
38. Taton TA. Boning up on biology. Nature. 2001; 412:491. [PubMed: 11484032]
39. Zhu H, Cao B, Zhen Z, Laxmi A, Li D, Liu S, Mao CB. Controlled growth and differentiation of mesenchymal stem cells on grooved films assembled from monodisperse biological nanofibers with genetically tunable surface chemistries. Biomaterials. 2011; 32:4744. [PubMed: 21507480]
40. Wang J, Wang L, Li X, Mao CB. Virus activated artificial ecm induces the osteogenic differentiation of mesenchymal stem cells without osteogenic supplements. Sci. Rep. 2013; 3:1242. [PubMed: 23393624]
41. Shi S, Gronthos S, Chen S, Reddi A, Counter CM, Robey PG, Wang C-Y. Bone formation by human postnatal bone marrow stromal stem cells is enhanced by telomerase expression. Nat. Biotechnol. 2002; 20:587. [PubMed: 12042862]
42. Bera S, Seb GTK, Hasirci V. Bone tissue engineering on patterned collagen films: An *in vitro* study. Biomaterials. 2005; 26:1997.
43. Datta N, Holtorf HL, Sikavitsas VI, Jansen JA, Mikos AG. Effect of bone extracellular matrix synthesized *in vitro* on the osteoblastic differentiation of marrow stromal cells. Biomaterials. 2005; 26:971. [PubMed: 15369685]

44. Hao L, Yang H, Du C, Fu X, Zhao N, Xu S, Cui F, Mao CB, Wang Y. Directing the fate of human and mouse mesenchymal stem cells by hydroxyl-methyl mixed self-assembled monolayers with varying wettability. J Mater. Chem. B. 2014; 2:4794.
45. Wiltfang J, Merten HA, Schlegel KA, Schultze-Mosgau S, Kloss FR, Rupprecht S, Kessler P. Degradation characteristics of alpha and beta tri-calcium-phosphate (TCP) in minipigs. J Biomed. Mater. Res. 2002; 63:115. [PubMed: 11870643]
46. Bruder SP, Fink DJ, Caplan AI. Mesenchymal stem cells in bone development, bone repair, and skeletal regeneration therapy. J Cell Biochem. 1994; 56:283. [PubMed: 7876320]
47. Castano-Izquierdo H, Alvarez-Barreto J, van den Dolder J, Jansen JA, Mikos AG, Sikavitsas VI. Pre-culture period of mesenchymal stem cells in osteogenic media influences their *in vivo* bone forming potential. J Biomed. Mater. Res. Part A. 2007; 82:129.
48. Oh S, Brammer KS, Li YSJ, Teng D, Engler AJ, Chien S, Jin S. Stem. Proc. Natl. Acad. Sci. USA. 2009; 106:2130. [PubMed: 19179282]
49. Lock J, Nguyen TY, Liu H. Nanophase hydroxyapatite and poly(lactide-co-glycolide) composites promote human mesenchymal stem cell adhesion and osteogenic differentiation *in vitro*. J Mater. Sci. Mater. Med. 2012; 23:2543. [PubMed: 22772475]
50. Chou YF, Dunn JC, Wu BM. *In vitro* response of MC3T3-E1 pre-osteoblasts within three-dimensional apatite-coated plga scaffolds. J Biomed. Mater. Res. B. 2005; 75:81.
51. Bourgeois B, Laboux O, Obadia L, Gauthier O, Betti E, Aguado E. Calcium-deficient apatite: A first *in vivo* study concerning bone in growth. J Biomed. Mater. Res. B. 2003; 65A:402.
52. Ramires PA, Romito A, Cosentino F, Milella E. The influence of titania/hydroxyapatite composite coatings on *in vitro* osteoblasts behaviour. Biomaterials. 2001; 22:1467. [PubMed: 11374445]
53. Ravichandran R, Venugopal J, Mukherjee S, Ramakrishna S. Precipitation of nanohydroxyapatite on PLLA/PBLG/collagen nanofibrous structures for the differentiation of adipose derived stem cells to osteogenic lineage. Biomaterials. 2012; 33:846. [PubMed: 22048006]
54. Venugopal J, Rajeswari R, Shayanti M, Ramakrishna S. Electrosprayed hydroxyapatite on polymer nanofibers to differentiate mesenchymal stem cells to osteogenesis. J Biomater. Sci. Polym. Ed. 2013; 24:170. [PubMed: 22370175]
55. Zhang YZ, Venugopal JR, Ramakrishna S, Lim CT. Enhanced biomineralization of osteoblasts on a novel electrospun biocomposite nanofibrous scaffold of hydroxyapatite/collagen/ chitosan. Tissue Eng. A. 2010; 16:1949.
56. Sacks MS, Gloeckner DC. Quantification of the fiber architecture and biaxial mechanical behavior of porcine intestinal submucosa. J Biomed. Mater. Res. A. 1999; 46:1.
57. Tanahashi M, Kokubo T. Apatite formation on surfaces of various substrates by a biomimetic process. Kagaku Kogyo. 1993; 44:703.
58. Tanahashi M, Matsuda T. Surface functional group dependence on apatite formation on self-assembled monolayers in a simulated body fluid. J Biomed. Mater. Res. 1997; 34:305. [PubMed: 9086400]
59. Jee SS, Thula TT, Gower LB. Development of bone-like composites via the polymer-induced liquid-precursor (PILP) process. Part 1: Influence of polymer molecular weight. Acta Biomater. 2010; 6:3676. [PubMed: 20359554]
60. Nudelman F, Pieterse K, George A, Bomans PHH, Friedrich H, Brylka LJ, Hilbers PAJ, With GD, Sommerdijk NAJM. The role of collagen in bone apatite formation in the presence of hydroxyapatite nucleation inhibitors. Nat. Mater. 2010; 9:1004. [PubMed: 20972429]
61. Wang L, Nancollas GH. Dynamics of biomineralization and biodemineralization. Met. Ions Life Sci. 2010; 4:413. [PubMed: 20721300]
62. Xie B, Nancollas GH. How to control the size and morphology of apatite nanocrystals in bone. Proc. Natl. Acad. Sci. USA. 2010; 107:22369. [PubMed: 21169505]
63. Spanos N, Misirlis DY, Kanellopoulou DG, Koutsoukos PG. Seeded growth of hydroxyapatite in simulated body fluid. J Mater. Sci. 2006; 41:1805.
64. Nancollas GH. The involvement of calcium phosphates in biological mineralization and demineralization processes. Pure Appl. Chem. 1992; 64:1673.

65. Gasik M, Keski-Honkola A, Bilotsky Y, Friman M. Development and optimisation of hydroxyapatite-β-TCP functionally gradated biomaterial. J Mech. Behav. Biomed. Mater. 2014; 30:266. [PubMed: 24361930]

66. Bohner M, Lemaitre J, Ring TA. Kinetics of dissolution of β-tricalcium phosphate. J Colloid Interface Sci. 1997; 190:37. [PubMed: 9241139]

67. Leong DT, Khor WM, Chew FT, Lim TC, Hutmacher DW. Characterization of osteogenically induced adipose tissue-derived precursor cells in 2-dimensional and 3-dimensional environments. Cells Tissues Organs. 2006; 182:1. [PubMed: 16651824]

68. Leong DT, Abraham MC, Rath SN, Lim TC, Chew FT, Hutmacher DW. Investigating the effects of preinduction on human adipose-derived precursor cells in an athymic rat model. Differentiation. 2006; 74:519. [PubMed: 17177849]

69. Leong DT, Nah WK, Gupta A, Hutmacher DW, Woodruff MA. The osteogenic differentiation of adipose tissue-derived precursor cells in a 3d scaffold/matrix environment. Curr. Drug Discov. Technol. 2008; 5:319. [PubMed: 19075612]

70. Cho HJ, Perikamana SKM, Lee JH, Lee J, Lee KM, Shin CS, Shin H. Effective immobilization of BMP-2 mediated by polydopamine coating on biodegradable nanofibers for enhanced *in vivo* bone formation. ACS Appl. Mater. Interf. 2014; 6:11225.

71. Wu F, Meng G, He J, Wu Y, Wu F, Gu Z. Antibiotic-loaded chitosan hhydrogel with superior dual functions: Antibacterial efficacy and osteoblastic cell responses. ACS Appl. Mater. Interf. 2014; 6:10005.

72. Lee HJ, Koh WG. Hydrogel micropattern-incorporated fibrous scaffolds capable of sequential growth factor delivery for enhanced osteogenesis of hMSCs. ACS Appl. Mater. Interf. 2014; 6:9338.

73. Liu X, Feng Q, Bachhuka A, Vasilev K. Surface modification by allylamine plasma polymerization promotes osteogenic differentiation of human adipose-derived stem cells. ACS Appl. Mater. Interf. 2014; 6:9733.

74. Li D, Sun H, Jiang L, Zhang K, Liu W, Zhu Y, Fangteng J, Shi C, Zhao L, Sun H, Yang B. Enhanced biocompatibility of PLGA nanofibers with gelatin/nano-hydroxyapatite bone biomimetics incorporation. ACS Appl. Mater. Interf. 2014; 6:9402.

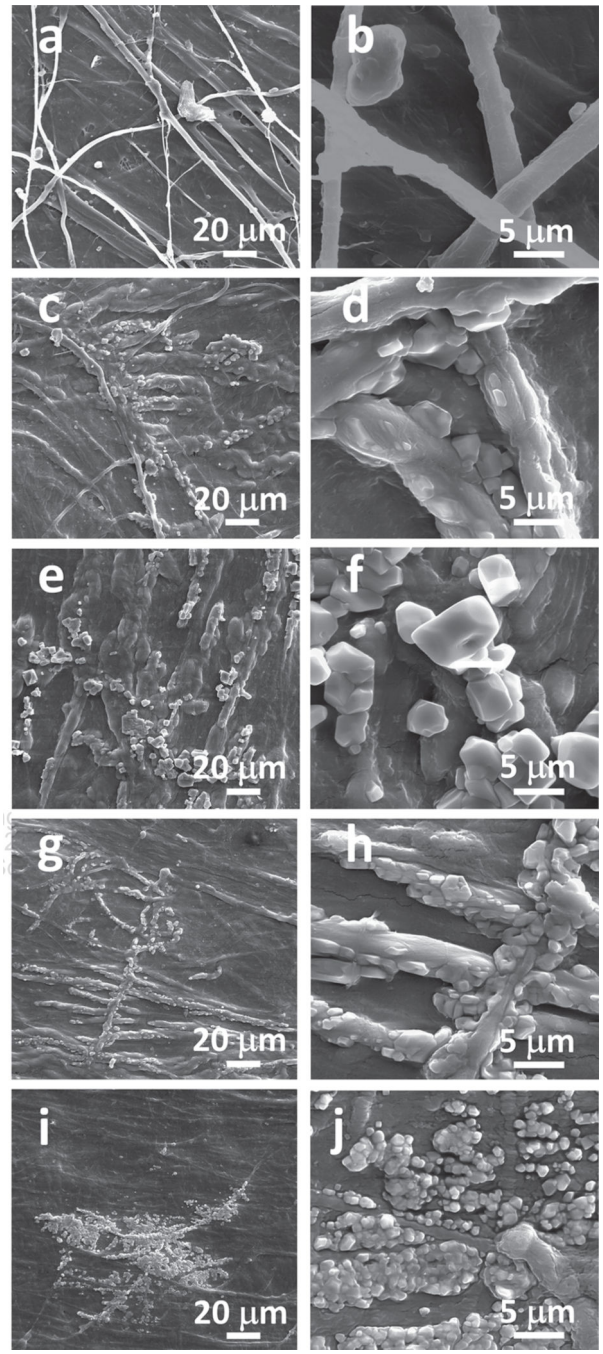

Figure 1.

Typical SEM images of the SIS membranes before and after they were incubated in 1.5 SBF solution at low magnification (left column) and high magnification (right column) for different times. (a, c, e, g) and (i) are typical low magnification images corresponding to the SIS membranes after being aged for 0, 0.5, 8, 24 and 96 h, respectively. (b, d, f, h) and (j) are high magnification images taken from the same membranes as (a, c, e, g) and (i), respectively. The typical SEM images of the surface of a blank SIS membrane (a and b)

show that the membrane is primarily made of densely packed nearly parallel type I collagen fibers and some collagen fibers are not parallel to each other.

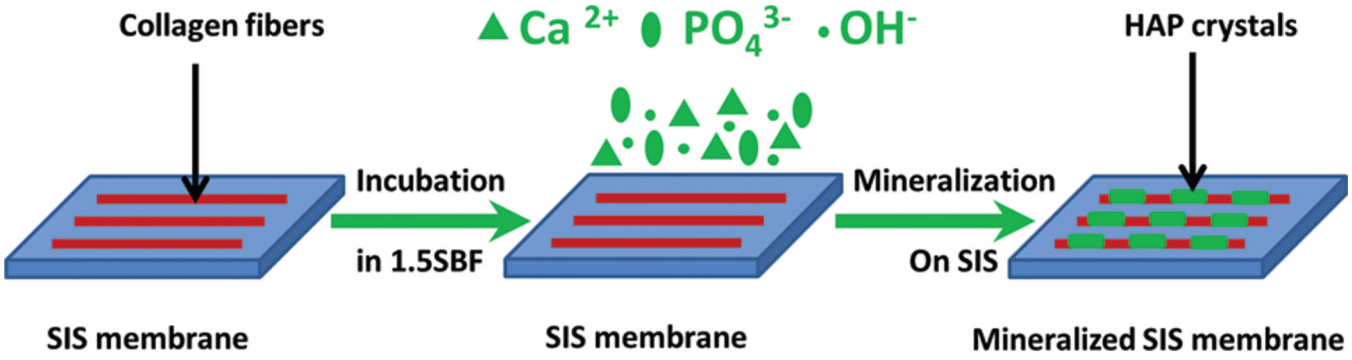

Figure 2.

XRD patterns of the surface of the SIS membranes after they were mineralized in 1.5 SBF solution for 0.5 h (A), 8 h (B), 24 h (C) and 96 h (D), respectively. A TCP peak is indicated by a red arrow in D.

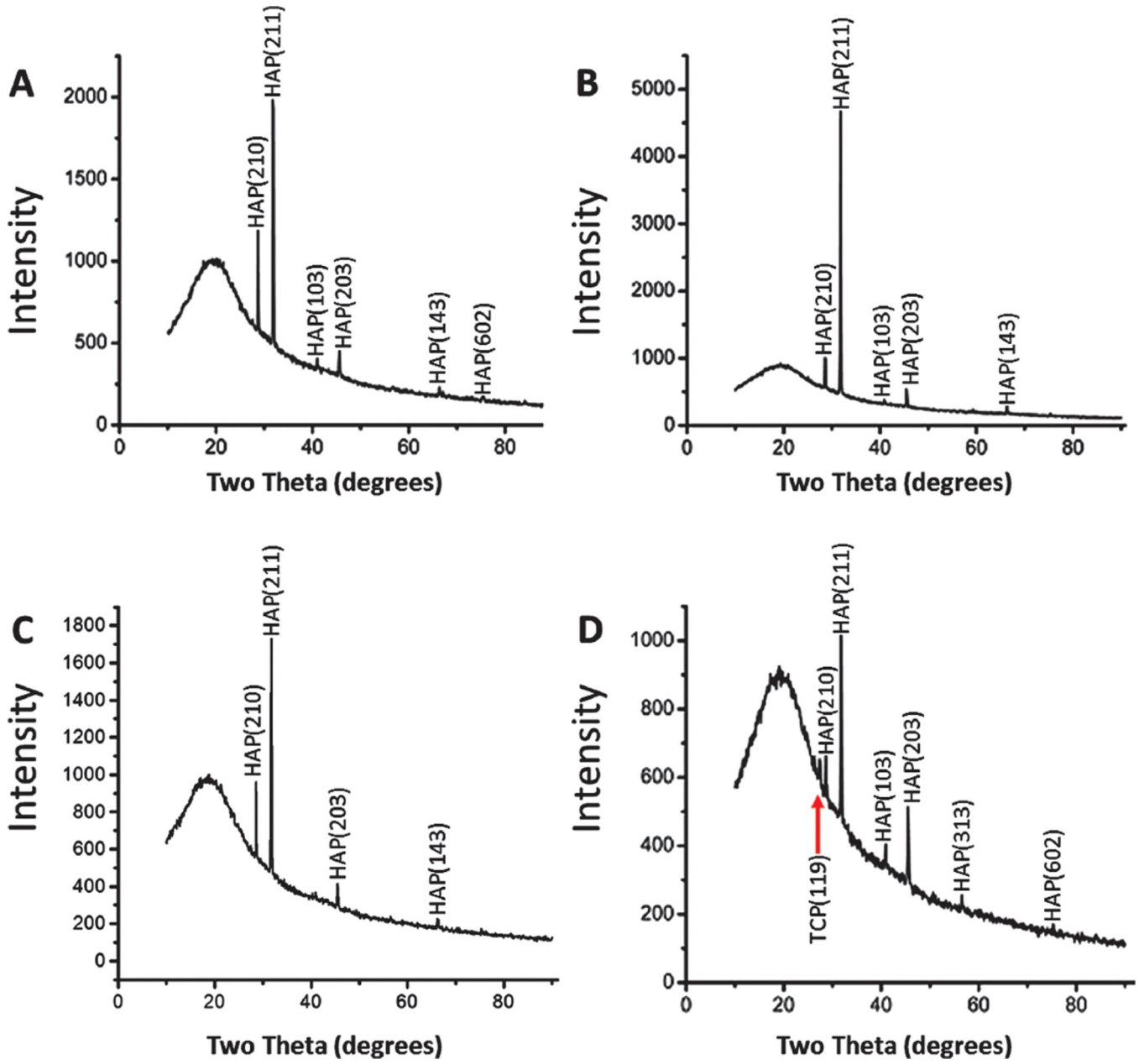

Figure 3.

Proliferation of MSCs on SIS membranes mineralized in 1.5 SBF for different times (0, 0.5, 8, 24, and 96 h) after being cultured for 1 day and 3 days. *, $p < 0.05$.

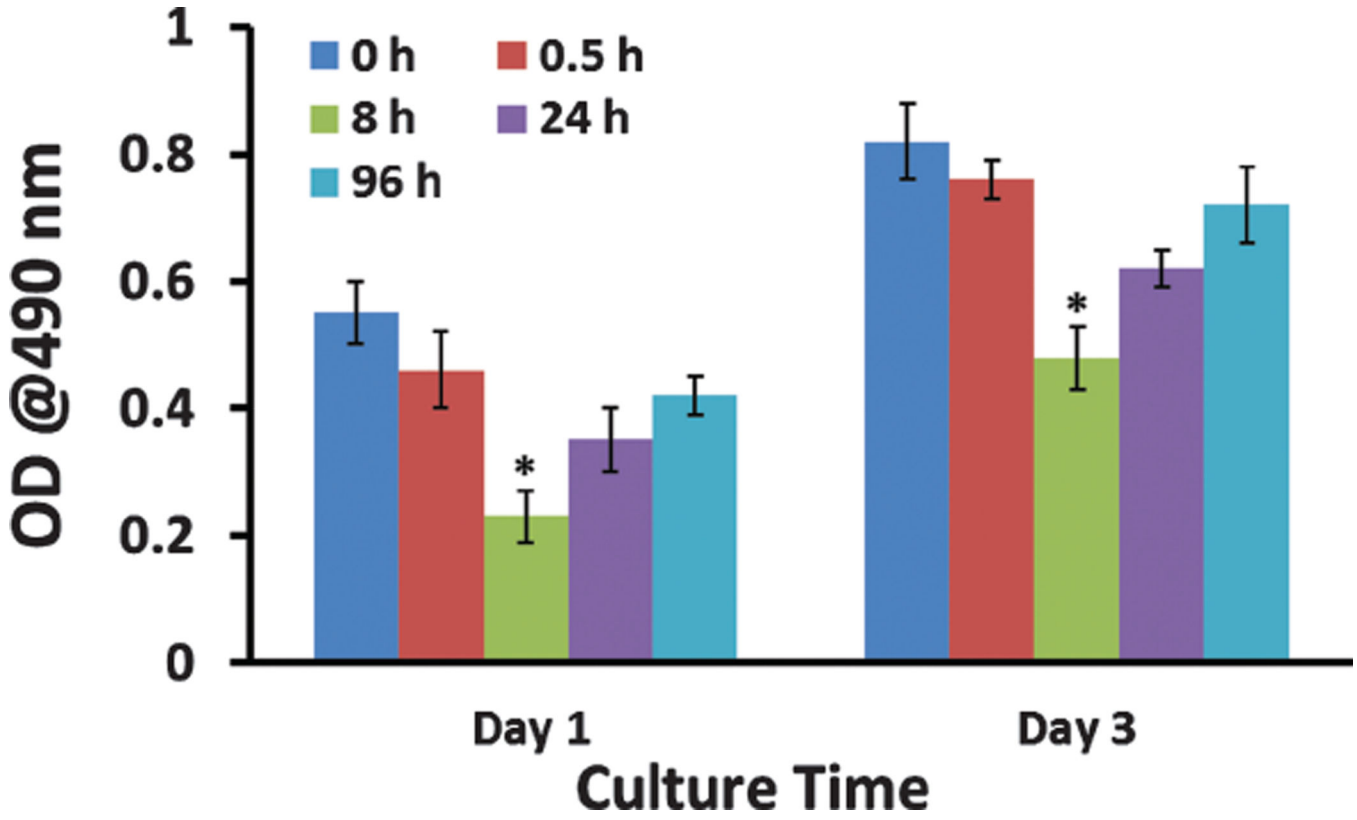

Figure 4.

Differentiation assay. (a) ALP activity of MSCs on SIS membranes mineralized in 1.5 SBF for different times (0, 0.5, 8, 24, and 96 h) after being cultured for 10 days in the osteogenic media. (b, c) Gene expression of OCN (b) and OPN (c) in MSCs on the SIS membranes mineralized in 1.5 SBF for different times (0, 0.5, 8, 24, and 96 h) after being cultured for 15 days in the osteogenic media. *, $p < 0.05$.

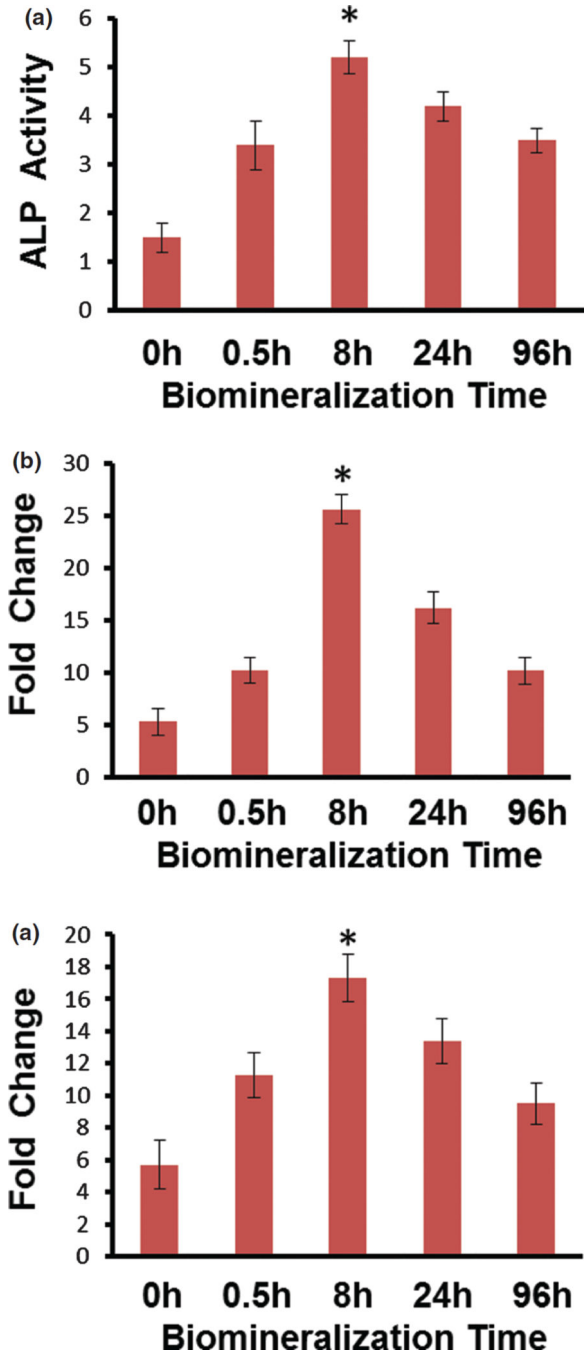

Scheme 1.

Principle of biomimetic nucleation and growth of hydroxylapatite crystals on the surface of SIS membrane from 1.5 SBF solution at the body temperature. The SIS membrane is incubated in 1.5 SBF at the body temperature to initiate the nucleation of HAP on the constituent collagen fibers. The HAP precursor ions (Ca^{2+}, PO_4^{3-} and OH^-) are deposited on the membrane surface to promote the nucleation of HAP.

Table I

Order, amounts, purities and molecular weights of reagents for preparing 1000 ml of 1.5 SBF.

Order	Reagent	Amount	Purity (%)	Molecular weight
1	NaCl	12.0525 g	99.5	58.4430
2	$NaHCO_3$	0.5325 g	99.5	84.0068
3	KCl	0.3375 g	99.5	74.5515
4	$K_2HPO_4 \cdot 3H_2O$	0.3465 g	99.0	228.2220
5	$MgCl_2 \cdot 6H_2O$	0.4665 g	98.0	203.3034
6	1.0 M-HCl	58.5 ml	–	–
7	$CaCl_2$	0.438 g	95.0	110.9848
8	Na_2SO_4	0.108 g	99.0	142.0428
9	Tris	9.177 g	99.0	121.1356
10	1.0 M-HCl	0–8 ml	–	–